

RICA - Radio Imaging Combination Analyzer

1 MILES LUCAS^{1,2}

2 ¹*Iowa State University, Ames, Iowa*

3 ²*National Radio Astronomy Observatory, Socorro, New Mexico*

4 ABSTRACT

5 1. INTRODUCTION

6 In radio synthesis imaging a common problem arising from interferometry is the lack of zero-spacing
7 data. Without this data, images lack total power information. Single dish radio telescopes retain
8 this total power information but lack the angular resolution capabilities of radio interferometers. To
9 solve this problem, astronomers combine the interferometry data with the total power data. This
10 report seeks to characterize the effectiveness of different combination methods and parameters.

11 The parameters analyzed were multiscale deconvolution versus normal Hogbom deconvolution, the
12 effect of single-dish size on the combination, masking, and number of total iterations (i.e. depth of
13 clean). One of the previous assumptions is that if the single-dish UV-coverage does not adequately
14 complement the interferometer UV-coverage, feathering will not be effective. Another assumption is
15 that simple point structures should not see much discrepancy in parameters or methods. Therefore,
16 more complex, fluffy structure ought to show more distinction in results.

17 There are four methods of combination that were tested. The first is CASA's *feather* task. The
18 process of feathering starts with regridding the lower resolution to the higher resolution image. Each
19 is then Fourier transformed and gridded, while the lower resolution data is scaled by the ratio of the
20 clean beams (high resolution/low resolution). The high-resolution grid is then added to this, scaled
21 by a weighting that starts at 0 and increases to 1 as the wavelength increases. This final combination
22 is then inverse Fourier transformed back into the image plane.

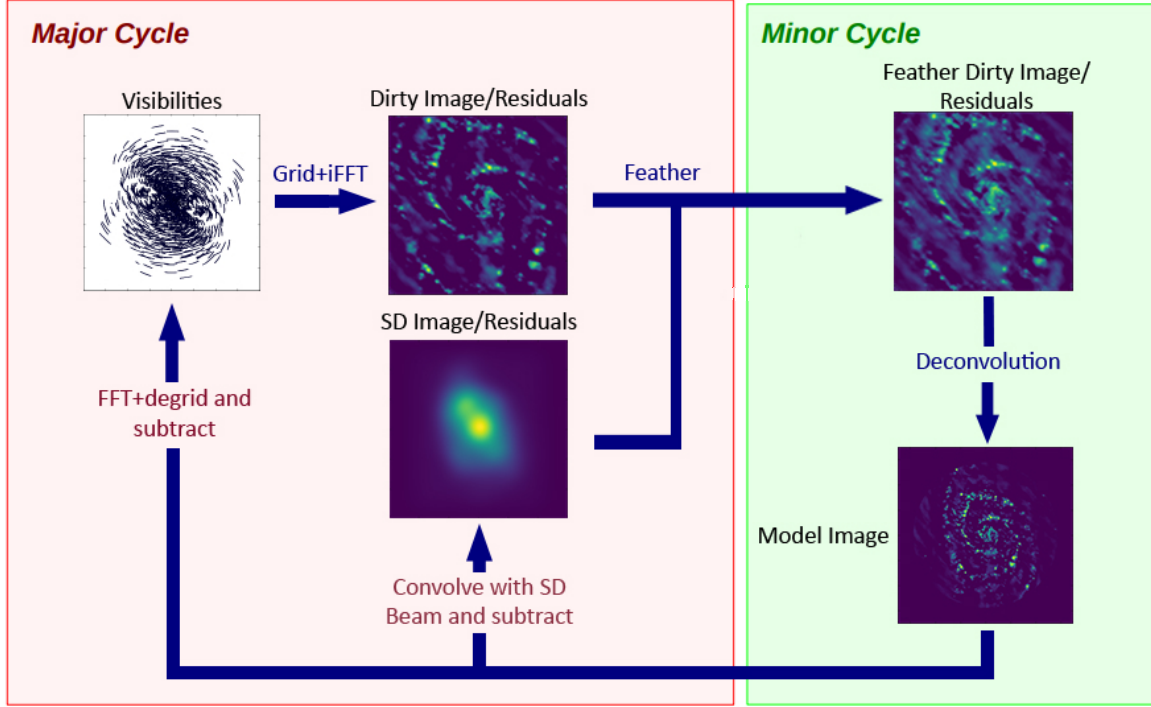


Figure 1. A flow chart describing the joint-deconvolution approach to combining interferometer and single dish data. Adapted from Rau, U. & Naik, N. 2018 (in prep).

23 The next method is using the total power image as the starting model in CASA's *tclean* task. In
 24 the Cotton-Schwab CLEAN algorithm (CSCLEAN), each major-cycle begins with a blank model
 25 image and constructs an image on it by using minor-cycle iterations. By using a starting model,
 26 this model is no longer blank, but is passed as a parameter. By using the total power image as the
 27 starting model, we can hope to retain the total power information through the CLEAN algorithm.

28 Another modification to the Cotton-Schwab cycle in order to combine images is by doing a modified
 29 joint deconvolution. In each major Cotton-Schwab cycle, the visibilities are gridded and inverse
 30 Fourier transformed to create an image residual, which is then feathered with the total power residual
 31 before deconvolving. The deconvolved model is then convolved with the single-dish beam and sub-
 32 tracted from the previous single-dish residual. The deconvolved model is also Fourier transformed,
 33 degridded, and subtracted from the visibilities to create a new residual image. These residuals are
 34 then degridded and transformed to finish the major cycle. See Figure 1 for a visual flowchart of the
 35 process.

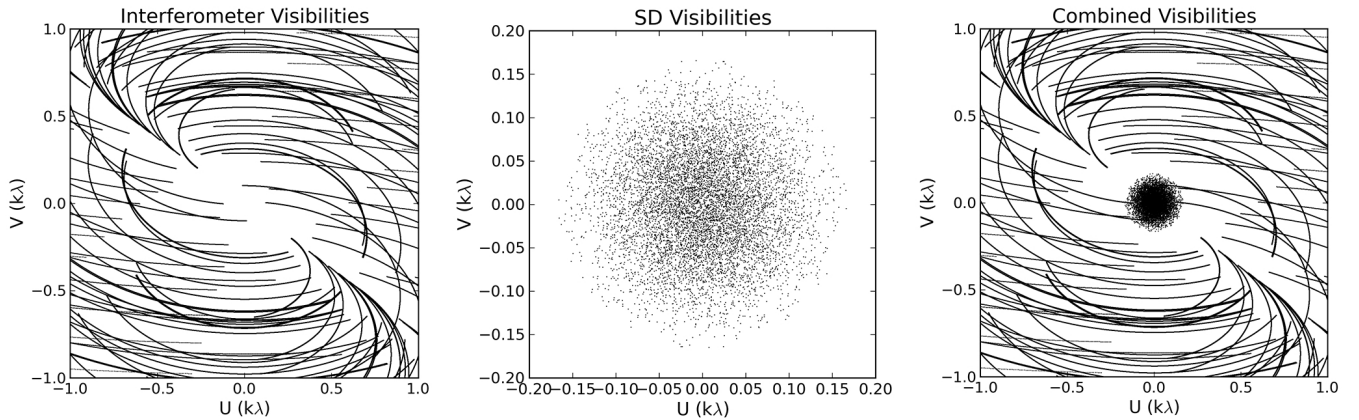


Figure 2. A look at how the visibilities are added through using *tp2vis* for a model simulated on the VLA A configuration. In the center of the interferometer image in the first plot shows sparsity that is filled in on the third plot. The second plot shows the approximation *tp2vis* makes of the single dish.

The last method of combination we use is *tp2vis*, which takes the total power image and spoofs a measurement set. The way *tp2vis* accomplishes this is by taking Fourier data from the total power image and sparsely sampling the Fourier data at close spacings (see Koda et al. 2011). This data can be concatenated with the interferometer data and deconvolved in *tclean*. Figure 2 shows how the single-dish is simulated and concatenated with the interferometer data. This should help fill the close-spacing gap created by the interferometer data and subsequently help increase total power information.

2. METHODS

In order to evaluate the different combination methods, a metric needed to be created and tested on a suite of models. The metrics used were CLEAN residuals, fidelity images, and a ratio of the power spectrum densities (PSD). The fidelities are given Equation 1

$$\text{Fidelity}(i, j) = \frac{|\text{Model}(i, j)|}{\max(|\text{Difference}(i, j)|, 0.7 \times \text{rms}(\text{Difference}))} \quad (1)$$

where model is the reference image and diff is the difference between the test and reference images (Pety et al. 2011, p.19). The exigence for using PSDs is that the zero-spacing power is readily visible for every image. By using these ratios, the closer the ratio is to 1.0 at short spacings (when compared

50 to the true model), the more accurate the combination. In addition, when compared with the total
 51 power image, it shows how much effective weight is given to the total power image in the combination.
 52 The ratio of the PSDs is given by [Equation 2](#)

$$\text{Ratio}(UV) = \frac{\text{Power}_{test}(UV)}{\text{Power}_{ref}(UV)} \cdot \frac{\text{BA}_{ref}}{\text{BA}_{test}} \quad (2)$$

$$\text{err}(UV) = \left(\frac{\text{Power}_{ref}(UV) + \text{Power}_{test}(UV)}{2} \right)^{-1} \quad (3)$$

53 where Power is the power from the PSD, BA is the beam area, *ref* refers to the reference image
 54 (model or SD), and *test* refers to whichever image is being tested. The uncertainty given is [Equation 3](#)
 55 such that the uncertainty is the reciprocal of the average of the PSDs.

56 Each combination was compared to both the true model and the single dish, total power image.
 57 Many models were tested with various extra parameters. Three models were generated from com-
 58 ponent lists. One has 4 point sources, one has a single Gaussian source, and one has a mixture of 4
 59 point sources, one very broad Gaussian, and on off-center, stronger Gaussian. There were also various
 60 models based off real structure, including M51 (based off an H- α image), Orion, RXJ1347, and a
 61 protoplanetary disk (PPD) simulation. [Figure 3](#) shows all of the models. It is important to note
 62 that these models have been regridded onto a common coordinate system that is not representative
 63 of the true astronomical targets. This was in effort to simplify the simulation process for creating
 64 measurement sets.

65 The code base for testing the effectiveness is hosted publicly for anyone to use¹. In the source code
 66 there are many scripts and methods to facilitate simulating, combining, and comparing. Every model
 67 is described in *src/_models.py* with a dictionary defining the simulation and *tclean* parameters. The
 68 pipeline for testing these models was as follows:

- 69 1. Simulate measurement set (MS) based on VLA configurations

¹ <https://gitlab.com/mileslucas/rica>

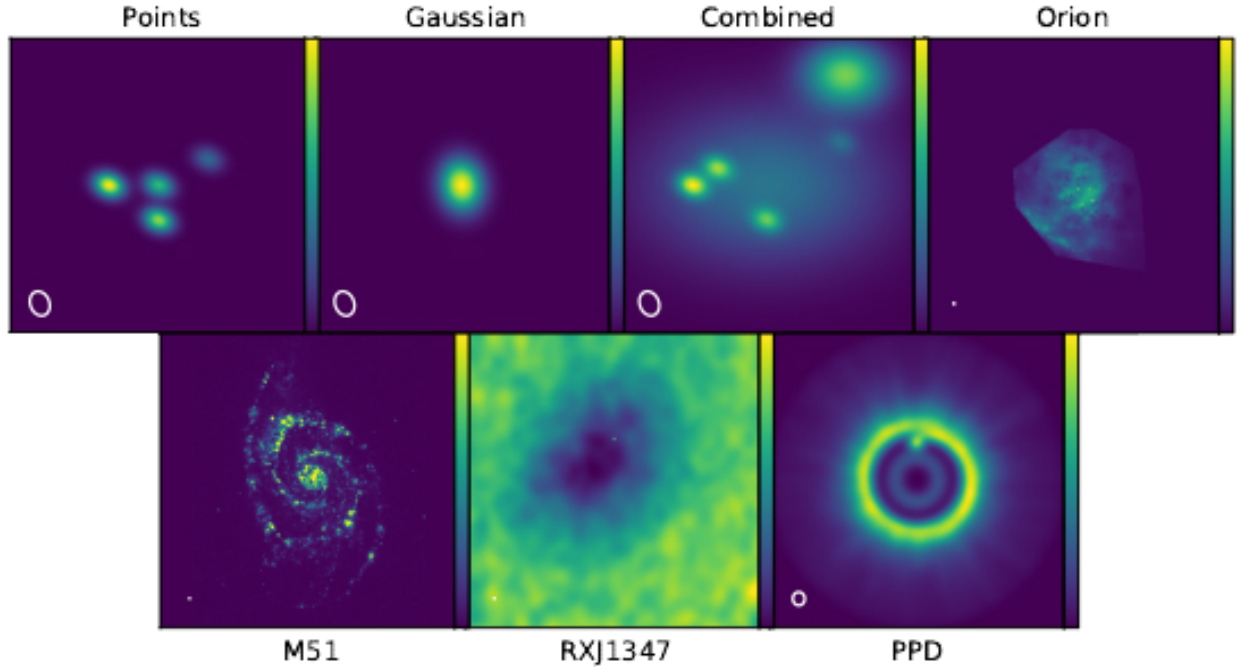


Figure 3. The models used for testing combination methods convolved with some restoring beam to show structure better.

- 70 2. Simulate single dish image by convolving model with Gaussian
- 71 3. Image the MS
- 72 4. Do the combinations (feather, startmodel, joint deconvolution, and tp2vis)
- 73 5. For each combination, do a comparison with the true model (convolved with the restoring
- 74 beam) and the single dish image
- 75 and is implemented in *src/pipeline.py*.

76 2.1. *Simulations and Deconvolution*

77 All simulations were done using the VLA for the telescope model except for the PPD simulation,
 78 which was done using *simalma* and was only simulated once. Each test model could define which
 79 of the VLA configurations to use, from A, B, BnA, C, CnB, D, and DnC. The spectral window for
 80 the simulations mimic the VLA C-band at 4.5 GHz to 5.5 GHz (central 5 GHz) with 101 channels at
 81 10 MHz intervals. The field observed was J2000 21h28m31.0 45°0'0''. The observation date and

82 time was 2018/06/01 at 12:00:00.0 UTC. The integration time was 10 s each with a total of 30 000 s.
 83 Finally, the data was corrupted with 1 mJy of simple noise.

84 The single dish images were created by taking the true model and convolving with a Gaussian
 85 equivalent to the single dish beam at the given frequency.

$$\text{FWHM}(\nu, D) = \frac{3.66 \times 10^8 \text{ m s}^{-1}}{\nu \cdot D} \quad (4)$$

86 Equation 4 gives the Gaussian kernel full-width half-maximum (FWHM) in radians for a frequency
 87 in Hz and dish diameter in meters. For instance, to simulate data from the Green Bank Telescope
 88 (GBT) with a dish diameter of 100 m at 5 GHz gives a FWHM of $2'31''$, which is in agreeance with
 89 values from the GBT proposer's guide². Note that this is not the most accurate equation for other
 90 telescopes, because there is a constant involved in this equation based off the taper-length of the
 91 telescope's feedhorns. In addition, these single dish images have 5×10^{-6} uniform noise added.

92 Each model defines its own parameters for cleaning. Appendix A lists every single parameter for
 93 each model. As a default, a model simulated in VLA D configuration has an image size of 64 with
 94 a cell size of $7.0''$. The restoring beam for the D configuration is approximately $20.41''$ by $15.60''$ so
 95 the cell accounts for half to a third of the beam width. In general, cleaning was done with very high
 96 numbers of iterations, relying on a threshold to stop the algorithm for consistency. This differs for
 97 the models tested at explicitly different cleaned levels.

98 2.2. Comparisons

99 Each comparison was ran with the same clean parameters for consistency. Because *feather* does
 100 not actively clean, it has its own set of parameters, but all of the models tested used the default
 101 parameters. After all the combination permutations were imaged, they were compared against the
 102 true model convolved with the restoring beam and the single dish image alongside the uncombined
 103 interferometer image. All of the ratio were saved into individual CSV files for further analysis. In

² p.9, <https://science.nrao.edu/facilities/gbt/proposing/GBTpg.pdf>

104 all, each model has 10 comparisons (5 against the models and 5 against the single-dish images) and
 105 4 separate cleans to perform.

106 In order to run a new model to test comparison methods, there are two general methods. If there
 107 exists a true model, simply add an entry to the models dictionary defining the simulation and clean
 108 parameters. It is also important to edit *src/simulate.py* to accommodate the new model. Follow the
 109 existing code base for guidance. It is also important to create a copy of the model and regrid it to
 110 the common coordinate system (use an existing model to retrieve the coordinate system). The model
 111 can then be ran through the pipeline along with any other models using *src/pipeline.py*.

112 If there is no true model, it is still useful to test and compare against the total power image, alone. In
 113 this case, using a cleaned image, a measurement set, and a total power image with the *src/combine.py*
 114 script will produce all of the combinations. These can then be compared using *src/compare.py*. It is
 115 possible to edit *src/pipeline.py* to accommodate special models, see how the PPD model is handled
 116 in the pipeline.

117 3. RESULTS

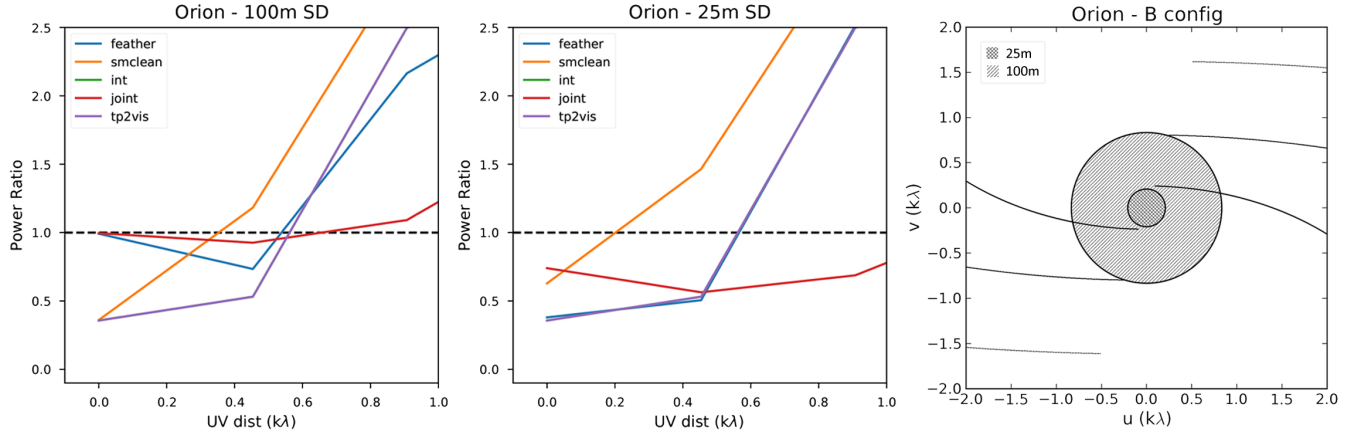


Figure 4. The left two plots are ratios for each combination method between two different single dish sizes. The horizontal line marks the ideal ratio for close UV spacing. The right plot shows the UV coverage of the interferometer with the coverage of the 100 m and 25 m single dishes overlaid.

118 For fidelity images and ratios of every comparison, see Appendix B. This section will only comment
 119 on a few models and comparison highlighting trends. The effect of single dish size was apparent on

120 the accuracy of combinations. Figure 4 shows how the ratios compare between the 100 m single dish
 121 size for the Orion model in B configuration and the 25 m single dish size of the same model.

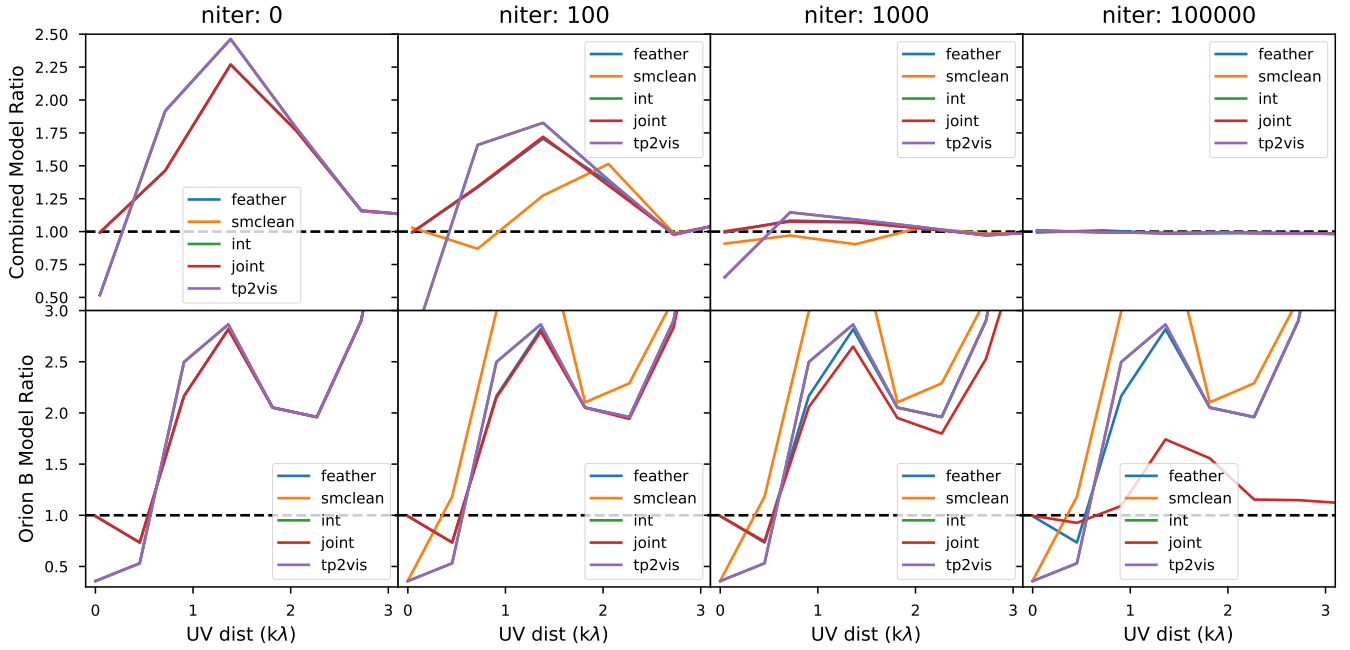


Figure 5. A comparison showing the effect on the combinations due to the depth of cleaning for two models, ‘combined’ and ‘orion-b’. The dashed black line represents the ideal ratio for the true model comparison.

122 Next, Figure 5 shows the effect that depth of cleaning has on the power ratios. Each row cor-
 123 responds to each model and each column is a depth of cleaning based on the number of iterations
 124 of deconvolution. The ‘combined’ model is a much simpler model than the ‘orion-b’ model. The
 125 parameters for each of these models with different iterations is shown in Appendix A.

4. CONCLUSION

126 From the results of Figure 4 it is notable that *feather* does not work as well for small single dish
 127 sizes. Both start model and joint deconvolution combination methods are able to do better than the
 128 plain interferometer with the small dish, but still do not reach that ideal ratio that is possible for
 129 the larger single dish. Looking at the coverage of the single dishes, the 25 m dish does not overlap
 130 with the interferometer data at all. This could be the reason why *feather* fails so much and why *joint*
 131

132 deconvolution and start model are not quite as good, either. Future studies might find the point at
 133 which there is enough overlay for each method to “succeed”.

134 From the results of [Figure 5](#) there are a few conclusions to be made. First, the joint deconvolution
 135 worked well regardless of the depth of cleaning for both models. Even completely dirty images had
 136 great total power information. After some amount of cleaning, *feather* quickly rose to the same
 137 level as joint deconvolution and in the ‘combined’ model, using a start model started working after
 138 some cleaning. In the simpler, ‘combined’ model, all combination methods converged at high enough
 139 iterations- even the interferometer image. However, for the more complex, ‘orion-b’ model, start
 140 model never converged and the values of the ratios remained erratic even at full cleaning depth.
 141 For future studies, it would be nice to try and see if joint deconvolution works for dirty images of
 142 many more models. In conjunction with the study on single dish size, there were no combinations
 143 that retrieved the total power information well from the dirty image due to insufficient single dish
 144 coverage³

145 Thank you to Dr. Kumar Golap and Dr. Takahiro Tsutsumi for their guidance and assistance.
 146 This work was funded by the National Science Foundation in partnership with the National Radio
 147 Astronomy Observatory and Associated Universities Incorporated.

148 *Software:* [CASA](#), [tp2vis](#) ([Koda et al. 2011](#))

REFERENCES

- | | |
|--|---|
| 149 Koda, J., Sawada, T., Wright, M. C. H., et al.
150 2011, ApJS, 193, 19,
151 doi: 10.1088/0067-0049/193/1/19 | 152 Pety, J., Gueth, F., & Guilloteau, S. 2011, ALMA
153 Memo #398 Impact of ACA on the Wide-Field
154 Imaging Capabilities of ALMA, Tech. rep. |
|--|---|

³ see ‘orion-b-25-n0’ ratio data

155

APPENDIX

156

A. MODEL PARAMETERS

157

The following table describes the parameters used for cleaning the model images. The only exception is the model ‘combined-sp’, which additionally uses specmode=’cube’ and nchan=-1 to facilitate cube imaging. For more details, look at the *src/_models.py* file, which this table is generated from.

158

159

Table 1. The parameters for every model ran through the pipeline

Name	Model	Config	SD size	imsize	cell	niter	cycleniter	threshold	deconvolver	scales	mask
points	points	VLA d	100 m	[64, 64]	7.00arcsec	100000	100	1e-5Jy	hogbom	No	
gauss	gauss	VLA d	100 m	[64, 64]	7.00arcsec	100000	100	1e-5Jy	hogbom	No	
combined	combined	VLA d	100 m	[64, 64]	7.00arcsec	100000	100	1e-5Jy	hogbom	No	
combined-n0	combined	VLA d	100 m	[64, 64]	7.00arcsec	0	100	1e-5Jy	hogbom	No	
combined-n100	combined	VLA d	100 m	[64, 64]	7.00arcsec	100	100	1e-5Jy	hogbom	No	
combined-n1000	combined	VLA d	100 m	[64, 64]	7.00arcsec	1000	100	1e-5Jy	hogbom	No	
combined-ms	combined	VLA d	100 m	[64, 64]	7.00arcsec	100000	100	1e-5Jy	multiscale	[0, 3, 10, 30]	No
m51	m51	VLA d	100 m	[128, 128]	7.00arcsec	100000	100	1e-12Jy	hogbom	No	
m51-ms	m51	VLA d	100 m	[128, 128]	7.00arcsec	100000	100	1e-12Jy	multiscale	[0, 3, 10, 30]	No
m51-b	m51	VLA b	100 m	[1400, 1400]	0.65arcsec	100000	100	1e-12Jy	hogbom	No	
m51-b-ms	m51	VLA b	100 m	[1400, 1400]	0.65arcsec	100000	100	1e-12Jy	multiscale	[0, 3, 10, 30]	No
orion-b	orion	VLA b	100 m	[700, 700]	0.65arcsec	100000	400	1e-9Jy	hogbom	Yes	
orion-b-n0	orion	VLA b	100 m	[700, 700]	0.65arcsec	0	100	1e-9Jy	hogbom	Yes	
orion-b-n100	orion	VLA b	100 m	[700, 700]	0.65arcsec	100	100	1e-9Jy	hogbom	Yes	

Table 1 continued on next page

Table 1 (*continued*)

Name	Model	Config	SD size	imsize	cell	niter	cycleniter	threshold	deconvolver	scales	mask
orion-b-n1000	orion	VLA b	100 m	[700, 700]	0.65arcsec	1000	100	1e-9Jy	hogbom		Yes
orion-b-ms	orion	VLA b	100 m	[700, 700]	0.65arcsec	100000	400	1e-9Jy	multiscale	[0, 3, 10, 50]	Yes
orion-b-25	orion	VLA b	25 m	[700, 700]	0.65arcsec	100000	400	1e-9Jy	hogbom		Yes
orion-b-25-n0	orion	VLA b	25 m	[700, 700]	0.65arcsec	0	100	1e-9Jy	hogbom		Yes
orion-b-25-n100	orion	VLA b	25 m	[700, 700]	0.65arcsec	100	100	1e-9Jy	hogbom		Yes
orion-b-25-n1000	orion	VLA b	25 m	[700, 700]	0.65arcsec	1000	100	1e-9Jy	hogbom		Yes
orion-b-25-ms	orion	VLA b	25 m	[700, 700]	0.65arcsec	100000	400	1e-9Jy	multiscale	[0, 3, 10, 30]	Yes
orion-c	orion	VLA c	100 m	[216, 216]	2.12arcsec	100000	400	1e-9Jy	hogbom		No
RXJ1347	RXJ1347	VLA a	100 m	[2268, 2268]	0.20arcsec	100000	100	1e-6Jy	hogbom		No
RXJ1347-masked	RXJ1347	VLA a	100 m	[2268, 2268]	0.20arcsec	100000	100	1e-6Jy	hogbom		Yes
ppd	ppd	ALMA	ACA	[192, 192]	0.01arcsec	100000	100	1e-7Jy	hogbom		No

160

B. MODEL RESULTS

161 For data tables of every single comparison, visit the [RICA repository](#).

162 **Fig. Set 1. Model Results**

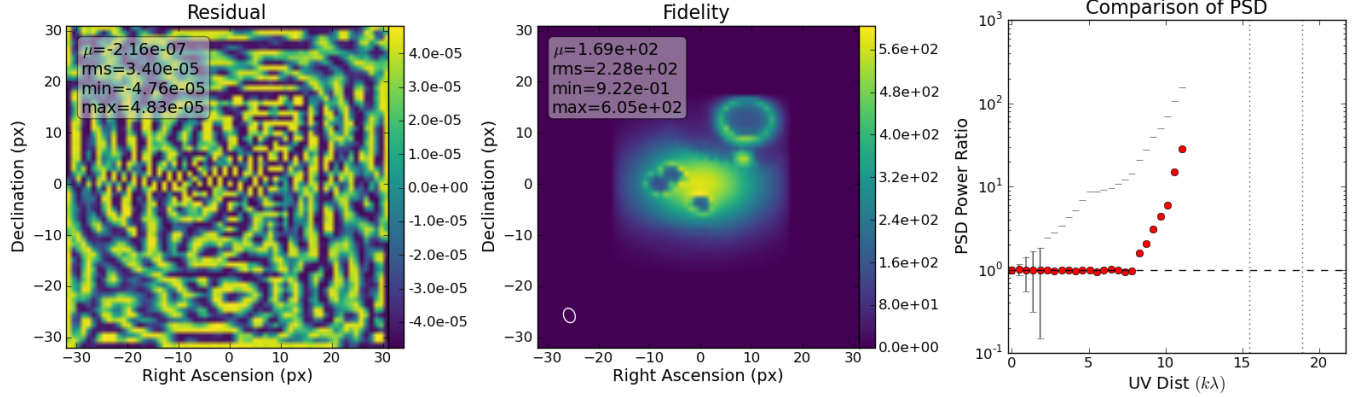


Figure 6. Comparison of feather combination to the true model for combined simulation. The ratio is Equation 2. The black ticks are error bars on a scaled uncertainty based on Equation 3. The vertical lines are the maximum UV distance of the interferometer at the longest and shortest wavelengths, respectively. The complete figure set (125 figures) is available at the [RICA repository](#).